Exclusive ρ^0 meson electroproduction from hydrogen at CLAS

CLAS Collaboration

C. Hadjidakis [a,b], M. Guidal [a], M. Garçon [c], J.-M. Laget [c], E.S. Smith [d],
M. Vanderhaeghen [d,e], G. Adams [ae], P. Ambrozewicz [n], E. Anciant [c], M. Anghinolfi [s],
B. Asavapibhop [x], G. Asryan [an], G. Audit [c], T. Auger [c], H. Avakian [d,b],
H. Bagdasaryan [ab], J.P. Ball [f], S. Barrow [o], M. Battaglieri [s], K. Beard [u],
M. Bektasoglu [aa,ab,am], M. Bellis [h], N. Benmouna [q], N. Bianchi [b], A.S. Biselli [h],
S. Boiarinov [d,t], B.E. Bonner [ag], S. Bouchigny [a,d], R. Bradford [h], D. Branford [m],
W.J. Briscoe [q], W.K. Brooks [d], V.D. Burkert [d], C. Butuceanu [e], J.R. Calarco [y],
D.S. Carman [aa], B. Carnahan [i], C. Cetina [q], S. Chen [o], P.L. Cole [i,d], A. Coleman [e],
D. Cords [d], P. Corvisiero [s], D. Crabb [al], H. Crannell [i], J.P. Cummings [ae], E. De Sanctis [b],
R. DeVita [s], P.V. Degtyarenko [d], L. Dennis [o], K.V. Dharmawardane [ab], K.S. Dhuga [q],
J.-P. Didelez [a], C. Djalali [ai], G.E. Dodge [ab], D. Doughty [j,d], P. Dragovitsch [o],
M. Dugger [f], S. Dytman [ad], O.P. Dzyubak [ai], H. Egiyan [d,e], K.S. Egiyan [an],
L. Elouadrhiri [j,d], A. Empl [ae], P. Eugenio [o], L. Farhi [c], R. Fatemi [al], R.J. Feuerbach [d],
T.A. Forest [ab], V. Frolov [ae], H. Funsten [e], S.J. Gaff [l], G. Gavalian [ab], G.P. Gilfoyle [ah],
K.L. Giovanetti [u], P. Girard [ai], C.I.O. Gordon [r], R.W. Gothe [ai], K.A. Griffioen [e],
M. Guillo [ai], M. Guler [ab], L. Guo [d], V. Gyurjyan [d], R.S. Hakobyan [i], J. Hardie [j,d],
D. Heddle [j,d], F.W. Hersman [y], K. Hicks [aa], H. Hleiqawi [aa], M. Holtrop [y], E. Hourany [a],
J. Hu [ae], C.E. Hyde-Wright [ab], Y. Ilieva [q], D. Ireland [r], M.M. Ito [d], D. Jenkins [ak],
H.-S. Jo [a], K. Joo [k,al], H.G. Juengst [q], J.H. Kelley [l], J. Kellie [r], M. Khandaker [z],
K.Y. Kim [ad], K. Kim [v], W. Kim [v], A. Klein [ab], F.J. Klein [i,d], A.V. Klimenko [ab],
M. Klusman [ae], M. Kossov [t], L.H. Kramer [n,d], S.E. Kuhn [ab], J. Kuhn [h], J. Lachniet [h],
J. Langheinrich [ai], D. Lawrence [x], T. Lee [y], Ji Li [ae], K. Livingstone [r], K. Lukashin [d],
J.J. Manak [d], C. Marchand [c], S. McAleer [o], J.W.C. McNabb [ac], B.A. Mecking [d],
J.J. Melone [r], M.D. Mestayer [d], C.A. Meyer [h], K. Mikhailov [t], R. Minehart [al],
M. Mirazita [b], R. Miskimen [x], L. Morand [c], S.A. Morrow [a,c], V. Muccifora [b],
J. Mueller [ad], G.S. Mutchler [ag], J. Napolitano [ae], R. Nasseripour [n], S.O. Nelson [l],
S. Niccolai [a,q], G. Niculescu [u,aa], I. Niculescu [u,q], B.B. Niczyporuk [d], R.A. Niyazov [d,ab],

M. Nozar [d], G.V. O'Rielly [q], M. Osipenko [s], K. Park [v], E. Pasyuk [f], G. Peterson [x],
S.A. Philips [q], N. Pivnyuk [t], D. Pocanic [al], O. Pogorelko [t], E. Polli [b], S. Pozdniakov [t],
B.M. Preedom [ai], J.W. Price [g], Y. Prok [al], D. Protopopescu [r], L.M. Qin [ab], B.A. Raue [n,d],
G. Riccardi [o], G. Ricco [s], M. Ripani [s], B.G. Ritchie [f], F. Ronchetti [b,af], P. Rossi [b],
G. Rosner [r], D. Rowntree [w], P.D. Rubin [ah], F. Sabatié [c,ab], K. Sabourov [l], C. Salgado [z],
J.P. Santoro [ak,d], V. Sapunenko [s], R.A. Schumacher [h], V.S. Serov [t], Y.G. Sharabian [d,an],
J. Shaw [x], S. Simionatto [q], A.V. Skabelin [w], L.C. Smith [al], D.I. Sober [i], M. Spraker [l],
A. Stavinsky [t], S. Stepanyan [d,an], B.E. Stokes [o], P. Stoler [ae], S. Strauch [q], M. Taiuti [s],
S. Taylor [ag], D.J. Tedeschi [ai], U. Thoma [p,d], R. Thompson [ad], A. Tkabladze [aa], L. Todor [ah],
C. Tur [ai], M. Ungaro [ae], M.F. Vineyard [aj,ah], A.V. Vlassov [t], K. Wang [al], L.B. Weinstein [ab],
H. Weller [l], D.P. Weygand [d], C.S. Whisnant [u,ai], M. Williams [h], E. Wolin [d], M.H. Wood [ai],
A. Yegneswaran [d], J. Yun [ab], L. Zana [y]

[a] *Institut de Physique Nucléaire ORSAY, Orsay, France*
[b] *INFN, Laboratori Nazionali di Frascati, Frascati, Italy*
[c] *CEA-Saclay, Service de Physique Nucléaire, F91191 Gif-sur-Yvette cedex, France*
[d] *Thomas Jefferson National Accelerator Facility, Newport News, VA 23606, USA*
[e] *College of William and Mary, Williamsburg, VA 23187-8795, USA*
[f] *Arizona State University, Tempe, AZ 85287-1504, USA*
[g] *University of California at Los Angeles, Los Angeles, CA 90095-1547, USA*
[h] *Carnegie Mellon University, Pittsburgh, PA 15213, USA*
[i] *Catholic University of America, Washington, DC 20064, USA*
[j] *Christopher Newport University, Newport News, VA 23606, USA*
[k] *University of Connecticut, Storrs, CT 06269, USA*
[l] *Duke University, Durham, NC 27708-0305, USA*
[m] *Edinburgh University, Edinburgh EH9 3JZ, United Kingdom*
[n] *Florida International University, Miami, FL 33199, USA*
[o] *Florida State University, Tallahassee, FL 32306, USA*
[p] *Physikalisches Institut der Universität Giessen, 35392 Giessen, Germany*
[q] *The George Washington University, Washington, DC 20052, USA*
[r] *University of Glasgow, Glasgow G12 8QQ, United Kingdom*
[s] *INFN, Sezione di Genova, 16146 Genova, Italy*
[t] *Institute of Theoretical and Experimental Physics, 117259 Moscow, Russia*
[u] *James Madison University, Harrisonburg, VA 22807, USA*
[v] *Kyungpook National University, Daegu 702-701, South Korea*
[w] *Massachusetts Institute of Technology, Cambridge, MA 02139-4307, USA*
[x] *University of Massachusetts, Amherst, MA 01003, USA*
[y] *University of New Hampshire, Durham, NH 03824-3568, USA*
[z] *Norfolk State University, Norfolk, VA 23504, USA*
[aa] *Ohio University, Athens, OH 45701, USA*
[ab] *Old Dominion University, Norfolk, VA 23529, USA*
[ac] *Penn State University, University Park, PA 15260, USA*
[ad] *University of Pittsburgh, Pittsburgh, PA 15260, USA*
[ae] *Rensselaer Polytechnic Institute, Troy, NY 12180-3590, USA*
[af] *Università di ROMA III, 00146 Roma, Italy*
[ag] *Rice University, Houston, TX 77005-1892, USA*
[ah] *University of Richmond, Richmond, VA 23173, USA*
[ai] *University of South Carolina, Columbia, SC 29208, USA*
[aj] *Union College, Schenectady, NY 12308, USA*
[ak] *Virginia Polytechnic Institute and State University, Blacksburg, VA 24061-0435, USA*
[al] *University of Virginia, Charlottesville, VA 22901, USA*

[am] *Sakarya University, Sakarya, Turkey*
[an] *Yerevan Physics Institute, 375036 Yerevan, Armenia*

Abstract

The longitudinal and transverse components of the cross section for the $ep \to e'p\rho^0$ reaction were measured in Hall B at Jefferson Laboratory using the CLAS detector. The data were taken with a 4.247 GeV electron beam and were analyzed in a range of x_B from 0.2 to 0.6 and of Q^2 from 1.5 to 3.0 GeV^2. The data are compared to a Regge model based on effective hadronic degrees of freedom and to a calculation based on Generalized Parton Distributions. It is found that, at our lowest x_B values, the transverse part of the cross section is well described by the former approach while the longitudinal part can be reproduced by the latter.

Understanding the precise nature of the confinement of quarks and gluons inside hadrons has been an ongoing problem since the advent, about 30 years ago, of the theory that governs their interactions, quantum chromodynamics (QCD). In particular, the transition between the high energy (small distance) domain, where quarks are quasi-free, and the low energy (large distance) regime, where they form bound states and are confined in hadrons, is still not well understood.

The analysis of elementary processes, such as the exclusive electroproduction of a meson or a photon on the nucleon in the few GeV range, allows one to study this transition. In the case of exclusive meson electroproduction, the longitudinal and transverse polarizations of the (virtual) photon mediating the interaction provide two qualitatively different pieces of information about the nucleon structure.

Longitudinal photons, whose transverse size is inversely proportional to their virtuality, truly act as a microscope. At sufficiently large Q^2, small distances are probed, and the asymptotic freedom of QCD justifies the understanding of the process in terms of partonic degrees of freedom and the use of perturbative QCD (pQCD) techniques. In particular, it has been recently shown [1,2] that the non-perturbative information can be factorized in reactions such as exclusive

vector meson electroproduction. Here the process can be described in terms of perturbative quark or gluon exchanges whose momentum, flavor, and spin distributions inside the nucleon are parametrized in terms of the recently introduced generalized parton distributions (GPDs) [3–5]. This is the so-called "hand-bag" diagram mechanism which is depicted in Fig. 1 (right diagram). At higher γ^*p center-of-mass energies, W, than considered in this Letter, 2-gluon exchange processes also intervene [2,6]. At low virtuality, Q^2, of the photon, hadronic degrees of freedom are more relevant and, above the nucleon resonance region, the process is adequately described in terms of meson exchanges Fig. 1 (left diagram).
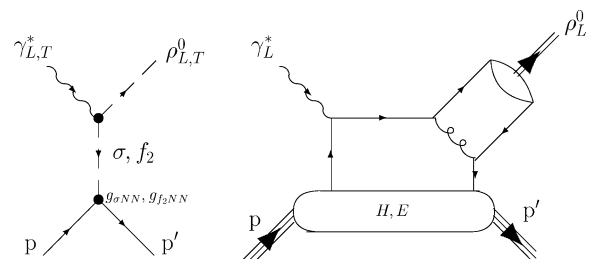

Fig. 1. The mechanisms for ρ^0 electroproduction at intermediate energies: at low Q^2 (left diagram) through the exchange of mesons, and at high Q^2 (right diagram) through the quark exchange "hand-bag" mechanism (valid for longitudinal photons) where H and E are the unpolarized GPD's.

E-mail address: guidal@ipno.in2p3.fr (M. Guidal).

For transverse photons, however, this description in terms of quarks and gluons is not valid. A factorization into a hard and soft part does not hold [1,2] and even at large Q^2, there is no dominance of a "handbag" mechanism as in Fig. 1. "Soft" (non-perturbative) and "hard" (perturbative) physics compete over a wider range of Q^2, and in practice it is necessary to take into account non-perturbative effects using hadron degrees of freedom. In order to access the fundamental partonic information when studying meson electroproduction processes, it is therefore highly desirable to isolate the longitudinal part of the cross section, which lends itself, at least at sufficiently high Q^2, to pQCD techniques and interpretation. In this approach, however, several questions remain to be answered. What is the lowest Q^2 where a perturbative treatment is valid? What corrections need to be applied to extend its validity to lower Q^2?

The aim of this Letter is to address these questions using the recent measurement of the longitudinal and transverse cross sections of the $ep \rightarrow e'p\rho^0$ reaction, carried out at Jefferson Laboratory using the CEBAF large acceptance spectrometer (CLAS) [7] in Hall B. This elementary process is one of the exclusive reactions on the nucleon which has the highest cross section, and for which the extraction of the longitudinal and transverse parts of the cross section can be accomplished using the ρ^0 decay angular distribution. On the theoretical side, formalisms and numerical estimates for both hadronic and partonic descriptions of the reaction have been developed, which can be compared to the transverse and longitudinal components of the cross section, respectively.

In the following, we will present the analysis results of the $ep \rightarrow e'p\rho^0$ reaction. Data were taken with an electron beam energy of 4.247 GeV impinging on an unpolarized liquid-hydrogen target. The integrated luminosity of this data set was about 1.5 fb^{-1}. The kinematic domain of the selected sample corresponds to Q^2 from 1.5 GeV^2 to 3.0 GeV^2. We analyzed data for W greater than 1.75 GeV, which corresponds to a range of x_B from 0.21 to 0.62. Our final data sample included about 2×10^4 $e'p\pi^+\pi^-$ events.

The ρ^0 meson decay to $\pi^+\pi^-$ was used to identify the reaction of interest. We identified the $ep \rightarrow e'p\pi^+\pi^-$ reaction using the missing mass technique by detecting the scattered electron, the recoil proton, and the positive pion. The electron was identified

as a negative track with reconstructed energy deposition in the calorimeter which was consistent with the momenta determined from magnetic analysis, in combination with a signal in the Cerenkov counter. The proton and pion were identified as positive tracks, whose combination of flight times and momenta corresponded to their mass. Fig. 2 (left plot) shows a typical missing mass distribution for $ep \rightarrow e'p\pi^+ X$ events. Events were selected by the missing mass cut $-0.03 < M_X^2 < 0.06$ GeV^2, consistent with a missing π^-. Fig. 2 (center) shows the resulting $\pi^+\pi^-$ invariant mass spectrum. The ρ^0 peak is clearly visible, sitting on a large non-resonant $\pi^+\pi^-$ background.

The unpolarized $ep \rightarrow e'p\pi^+\pi^-$ reaction is fully defined by seven independent kinematical variables which we have chosen as: Q^2 and x_B, which define the virtual photon kinematics; t, the invariant squared momentum transfer between the virtual photon and the final pion pair (i.e., the ρ^0 meson when this particle is produced); $M_{\pi^+\pi^-}$, the invariant mass of the $\pi^+\pi^-$ system; θ_{hel} and ϕ_{hel}, the π^+ decay angles in the $\pi^+\pi^-$ rest frame; and Φ, the azimuthal angle between the hadronic and leptonic planes. The CLAS acceptance and efficiency were calculated for each of these 7-dimensional bins using a GEANT-based simulation of several hundred million events. In the limit of the finite size of the bins, this method for the acceptance calculation is independent of the event generator. The event distributions were generated according to Ref. [8], which includes the three main contributions above the resonance region to the $e'p\pi^+\pi^-$ final state: diffractive $ep \rightarrow e'p\rho^0$, t-channel $ep \rightarrow e'\Delta^{++}\pi^-$, and non-resonant (phase space) $ep \rightarrow e'p\pi^+\pi^-$. Each of these contributions to the event generator was matched to the world's data on differential and total cross sections, and then extrapolated to our kinematical domain. In order to estimate the reliability of the acceptance calculation, we varied the weight of these three contributions to the event generator and found the variations of our results to be less than 6%, which is the systematic error that we attributed to this part of the analysis. We were then able to extract a total cross section for the $ep \rightarrow e'p\pi^+\pi^-$ channel in good agreement with world's data where the kinematics overlapped. The event generator also includes radiative effects following the Mo and Tsai prescription [9] so that radiative corrections could be applied in each (Q^2, x_B) bin.
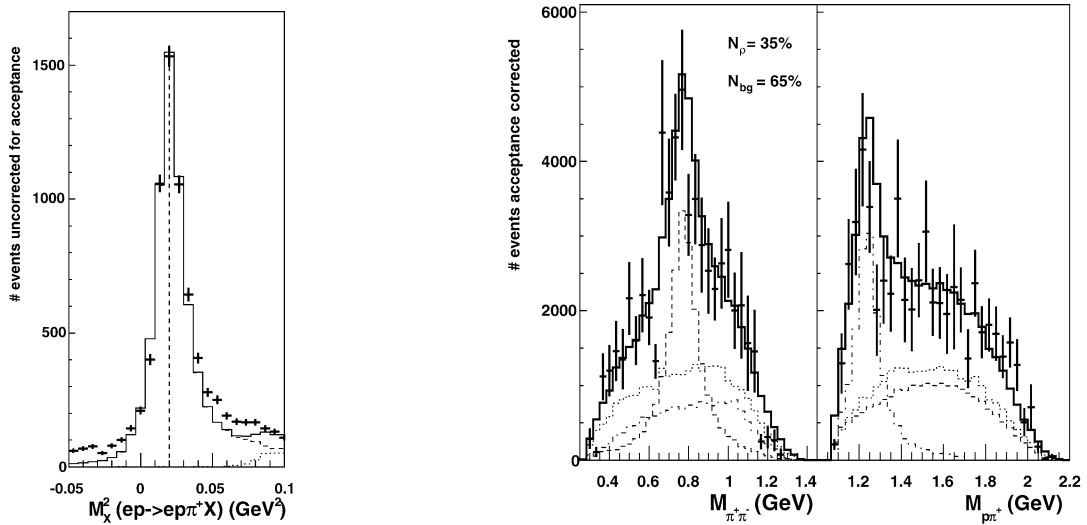
Fig. 2. Left plot: an example of a squared missing mass $M_X^2(ep \rightarrow e'p\pi^+X)$ spectrum (for a scattered electron momentum between 1.9 and 2.2 GeV). Points with error bars show the experimental data and the solid lines represent the results of simulations for the channels $e'p\pi^+\pi^-$ (dashed line), $e'p\pi^+\pi^-\pi^0$ (dotted line) and the sum of the two (solid line). The vertical dashed line is located at the missing mass squared of a pion. Central and right plots: an example of the $\pi^+\pi^-$ and $p\pi^+$ invariant masses, respectively (for the interval $1.63 < Q^2 < 1.76$ GeV^2 and $0.28 < x_B < 0.35$). Points with error bars show the experimental data and the lines correspond to the results of fits for the channels $ep \rightarrow e'p\rho^0$ (dashed line), $ep \rightarrow e'\Delta^{++}\pi^-$ (dash-dotted line), non-resonant $ep \rightarrow e'p\pi^+\pi^-$ (dotted line) and the sum of the three processes (solid line).

The main difficulty in determining the ρ^0 yield stems from its large width ($\Gamma_{\rho^0} \sim 150$ MeV), which does not allow for a unique determination of the separate contributions due to the resonant ρ^0 production and non-resonant $\pi^+\pi^-$ pairs. We simultaneously fitted the two 3-fold differential cross sections $d^3\sigma/dQ^2 dx_B dM_{\pi^+\pi^-}$ and $d^3\sigma/dQ^2 dx_B dM_{p\pi^+}$ to determine the weight of the three channels mentioned earlier, leading to the $e'p\pi^+\pi^-$ final state (see Fig. 2, central and right plots). The mass spectra of the ρ^0 and Δ^{++} are generated according to standard Breit–Wigner distributions and the non-resonant $p\pi^+\pi^-$ final state according to phase space. This background estimation procedure, along with the CLAS acceptance modeling, is one of the dominant sources of systematic uncertainty which, in total, ranges from 10 to 25%. More sophisticated shapes for the ρ^0 mass spectra were also investigated but led to consistent numbers of ρ^0's within these error bars.

The final step of the analysis consisted in separating the longitudinal and the transverse parts of the $ep \rightarrow e'p\rho^0$ cross section. The determination of these two contributions was accomplished under the assumption of s-channel helicity conservation (SCHC) [10]. This hypothesis states, in simple terms, that the helicity of

the virtual photon is directly transferred to the vector meson. The SCHC hypothesis originates from the vector meson dominance model which identifies vector meson electromagnetic production as an elastic process without spin transfer.

The validity of the SCHC hypothesis, which is only applicable at small momentum transfer t, can be tested experimentally through the analysis of the azimuthal angular distribution. We found that the r_{1-1}^{04} ρ^0 decay matrix element [11], which can be extracted from the ϕ_{hel} dependence, was compatible with zero at the 1.7 sigma level. We also found that the σ_{TT} and σ_{TL} cross sections, which can be extracted from the Φ dependence, were, respectively, $10.6 \pm 11.8\%$ and $0.4 \pm 5.4\%$ of the total cross section. They are therefore consistent with zero, as they should be if SCHC is valid and, in any case, do not represent potential large violations of SCHC. Let us also note that all previous experiments on electromagnetic production of ρ^0 on the nucleon are consistent with the dominance of s-channel helicity conserving amplitudes (the helicity-flip amplitudes which have been reported [12–15] never exceeded 10–20% of the helicity non-flip amplitudes). We can therefore safely rely on SCHC for our analysis.
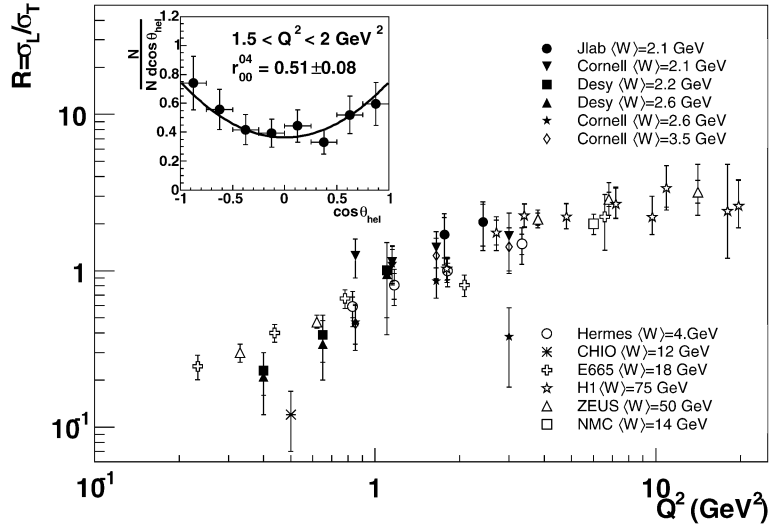
Fig. 3. The ratio $R = \sigma_L/\sigma_T$ as a function of Q^2 for ρ^0 meson electroproduction on the nucleon. The other data are from [12–20]. The insert shows one of our $\cos\theta_{\mathrm{hel}}$ distributions with a fit to determine r_{00}^{04}.

The decay angular distribution of the π^+ in the ρ^0 rest frame can be written as [11]:

$$W(\cos\theta_{\mathrm{hel}}) = \frac{3}{4}\big[1 - r_{00}^{04} + \big(3r_{00}^{04} - 1\big)\cos^2\theta_{\mathrm{hel}}\big], \quad (1)$$

where r_{00}^{04} represents the degree of longitudinal polarization of the ρ meson. Under the assumption of SCHC, the ratio of longitudinal to transverse cross sections is

$$R_\rho = \frac{\sigma_L}{\sigma_T} = \frac{1}{\epsilon}\frac{r_{00}^{04}}{1 - r_{00}^{04}}, \quad (2)$$

where ϵ is the virtual photon transverse polarization. r_{00}^{04} was extracted from the fit of the background-subtracted $\cos\theta_{\mathrm{hel}}$ distributions following Eq. (1) as illustrated in the insert in Fig. 3, and was used in Eq. (2) to determine R_ρ.

Due to limited statistics in the CLAS data, this procedure could be performed only for the two Q^2 points which are shown on Fig. 3. We see that our points are compatible with the existing world's data. We then have fitted the Q^2 dependence of R_ρ including, in order to take into account a potential W dependence of the ratio R, only the world's data in the W domain close to ours ($W \approx 2.1$ GeV) [12,16]. The following parametrization, whose power form is motivated by the perturbative PQCD prediction that σ_T is power

suppressed with respect to σ_L, was found:

$$R_\rho = (0.75 \pm 0.08) \times (Q^2)^{1.09 \pm 0.14}. \quad (3)$$

It is customary to define the reduced cross section for ρ meson production as the electroproduction cross section divided by the flux of virtual photons:

$$\sigma_T + \epsilon\sigma_L = \frac{1}{\Gamma_V(Q^2, x_B)} \times \frac{d^2\sigma^{\mathrm{ep}}}{dQ^2\,dx_B}, \quad (4)$$

where the virtual photon flux is given by:

$$\Gamma_V(Q^2, x_B) = \frac{\alpha}{8\pi}\frac{Q^2}{M_p^2 E_e^2}\frac{1 - x_B}{x_B^3}\frac{1}{1 - \epsilon}. \quad (5)$$

In this notation, and in Fig. 4, the longitudinal and transverse σ_T and σ_L cross sections are integrated over t, Φ, θ_{hel}, and ϕ_{hel}. The t dependence of $\sigma_T + \epsilon\sigma_L$ can be parametrized by $e^{-b|t-t_{\min}|}$ for the range $0 < -(t - t_{\min}) < 1$ GeV^2, where $-t_{\min}$ is the smallest value of momentum transfer for a given kinematic bin. We measured the exponential slope b to range from 1.19 to 1.74 GeV^{-2} for x_B between 0.31 and 0.52. Our data actually extended up to $-(t - t_{\min}) = 2$ GeV^2, depending on x_B and Q^2.

The longitudinal and transverse cross sections are plotted in Fig. 4 as a function of Q^2 for four bins centered at x_B of 0.31, 0.38, 0.48, and 0.52. These values correspond to W values of 2.2, 2.0, 1.9, and 1.85 GeV,
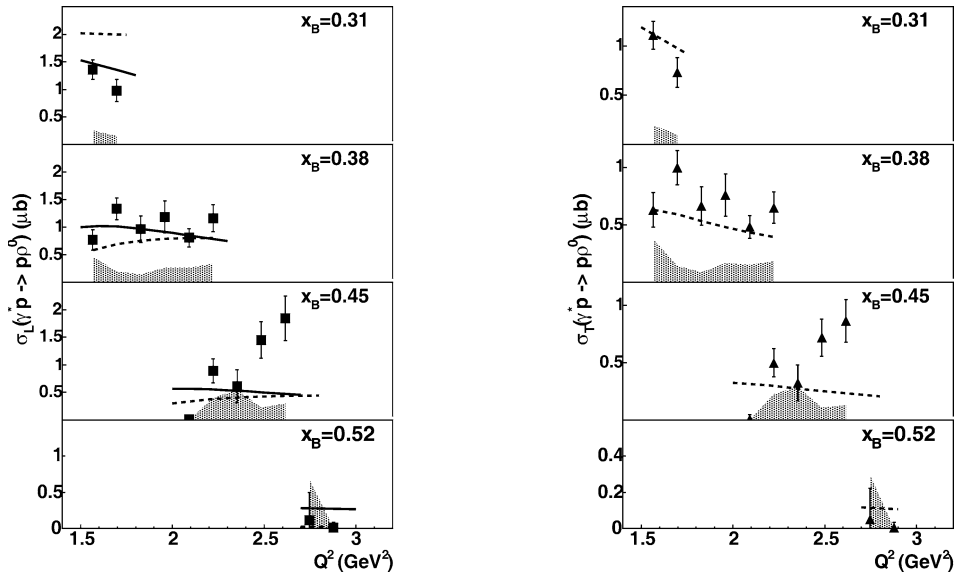
Fig. 4. Cross sections σ_L (left) and σ_T (right) for $ep \to e'p\rho^0$ as a function of Q^2 as measured in this experiment. The dotted line represents the Regge model of Refs. [21,22] while the solid line describes the GPD model of Refs. [6,23]. The systematic error is indicated by the shaded zones at the bottom of the plots.

respectively. The data are compared to two theoretical approaches. The first one is based on hadronic degrees of freedom with meson Regge trajectory exchanges in the t-channel (as illustrated in Fig. 1, left graph). This approach has been successful in describing, with very few free parameters, essentially all of the available observables of a series of forward exclusive reactions in photo- and electroproduction of pseudoscalar mesons ($\pi^{0,\pm}$, K^+ [24], η, η' [25]) above the resonance region. For the ρ^0, ω, ϕ vector mesons, as well as for Compton scattering, such an approach has been recently developed in Refs. [21,22,26]. In the case of ρ^0 electroproduction, the contributing meson trajectories are the σ, f_2, and Pomeron, the latter being negligible in the W region investigated in this experiment. This Regge model was normalized by adjusting the σ and f_2 meson–nucleon couplings to reproduce existing photoproduction data (see, for instance, Ref. [27]). There is little freedom in the choice of parameters when one uses data from all three ρ^0, ω, and ϕ channels, which together constrain all photoproduction parameters. The only remaining free parameters for the electroproduction case are the squared mass scales of the meson monopole form factors at the electromagnetic vertices for the diagrams of Fig. 1 (left plot). They have been determined from the Q^2 de-

pendence of the world's data, in particular from the Cornell [16] and HERMES [31] experiments, to be approximatively 0.5 GeV^2, in accordance with known meson form factor mass scales.

As shown in Fig. 4, this Regge model provides a fair description of the transverse and longitudinal cross sections at our lowest x_B values. There is some discrepancy at large values of x_B. Several reasons can be invoked for this: first of all, in general. Regge theory is valid at high energies and its application is all the less valid as one goes to low W (i.e., large x_B). More specifically, some s-channel nucleonic resonances decaying into $\rho^0 p$ may contribute, a process which is not taken into account in the Regge t-channel approach, and might explain the missing strength in this particular kinematical domain. Also, the $t_{\min}$ value corresponding to these "high" x_B values is quite large ($t_{\min} \approx -0.7$ GeV^2 at $x_B = 0.45$ and $Q^2 = 2.3$ GeV^2, while it decreases as one goes to smaller x_B values); Regge theory is essentially a small t theory and corrections might be sizeable at large t. In the same spirit. SCHC, which could be tested only globally, i.e., integrated over t, due to lack of sufficient statistics, might also be less valid. The Regge calculation was also done for the higher energy Cornell [16] and HERMES [31] data, where general agreement is found as well.

We now turn to the handbag diagram approach Fig. 1 (right plot), which is based on the QCD factorization between a "hard" process (the interaction between a quark of the nucleon and the virtual photon, along with a one-gluon exchange for the formation of the final meson) and a "soft" process (the parametrization of the partonic structure of the nucleon in terms of GPD's). As mentioned in the introduction, this approach is only valid at sufficiently large Q^2 when the longitudinal cross section dominates the QCD expansion in powers of $1/Q^2$. Unfortunately, the value of Q^2 at which the "handbag" mechanism becomes valid is unknown, and especially for meson electroproduction, it must be determined experimentally.

The calculation of the handbag diagram has been done at leading order in α_s and leading twist accuracy. In the case of ρ^0 production, only the unpolarized GPD's H and E contribute to the amplitude of the reaction. In the calculation, shown in Fig. 4, we neglect the contribution due to the GPD E because it is proportional to the 4-momentum transfer between the incoming virtual photon and the outgoing meson, and our data cover mostly small momentum transfers. For the GPD H we use the parametrization based on "double distributions" (with $b_{\mathrm{val}} = b_{\mathrm{sea}} = 1$) of Refs. [6,23,28] for the x and ξ dependencies, without D-term [23,29,30] and with a factorized exponential for the t dependence whose slope is given by our data. The other ingredient entering the (leading order) calculation of the handbag diagram is the treatment of the strong coupling constant α_s between the quarks and the gluon. It has been "frozen" to a value of 0.56, as determined by QCD sum rules [32]. The freezing of the strong coupling constant α_s is an effective way to average out non-perturbative effects at low Q^2 and is supported by jet-shape analysis of the infrared coupling [33].

As mentioned earlier, the handbag diagram calculation can only be compared with the longitudinal part of the cross section. Fig. 4 shows a good agreement between the calculation and the data at the low x_B values. The same reasons as for the Regge model discussed above can be invoked to explain the discrepancy between the data and the handbag calculation for the two highest x_B bins: on the one hand, nucleonic resonance "contamination" cannot be excluded and, on the other hand, large t_{min} values at large x_B render the neglect of the GPD E less valid and makes the calculation

more sensitive to higher twist corrections. Variations in reasonable ranges of the parameters (b_{val} and b_{sea} and addition or not of the "D-term") entering the GPD were studied, and results were found to be stable at the 50% level. This provides confidence in the stability, reliability, and validity of the calculation based on the prescription of a "frozen" α_s. Let us also note that this calculation reproduces reasonably well the HERMES data [31], which were taken at neighboring kinematics.

A signature of the handbag mechanism is that, independent of any particular GPD parametrization adopted, the (reduced) cross sections should follow a $1/Q^6$ dependence at fixed t and x_B. In this analysis, due to the lack of statistics, σ_L is integrated over t, which means that it is proportional to t_{min}, this latter variable changing as a function of Q^2. This $1/Q^6$ scaling behavior at fixed t and x_B can therefore not be directly observed in our data, which is modified by the (trivial) kinematical Q^2 dependence of t_{min}. Nevertheless, agreement between the data and the GPD calculation, which also contains this trivial t_{min} dependence, should be interpreted as confirmation of the leading order prediction based on the "handbag" diagram.

In conclusion, we have presented here a first exploration of exclusive vector meson electroproduction on the nucleon in a region of Q^2 between 1.5 and 3.0 GeV^2 and x_B between 0.2 and 0.6, which is a kinematical domain barely explored. At our lowest x_B values, the Regge model, based on "economical" hadronic degrees of freedom and which already describes all other existing vector meson photo- and electro-production data above the resonance region, is able to describe the transverse cross section data. Identically, at our lowest x_B values, the more fundamental "handbag" approach, with a standard parametrization of the GPD H and the extrapolation to low Q^2 by an effective freezing of α_s, provides a fair description of the longitudinal part of the cross section. Therefore, in some region of the x_B, Q^2 phase space, it seems possible to understand the longitudinal part of the ρ meson production cross section in a pQCD framework, which potentially gives access to GPDs, while the transverse cross section, for which no factorization between soft and hard physics exists, can be described in terms of meson exchanges. These tentative conclusions need of course to be confirmed by a more extensive and thor-

ough exploration of the x_B, Q^2 phase space which is currently under way with a much larger data set [34].

Acknowledgements

References

[1] J.C. Collins, L. Frankfurt, M. Strikman, Phys. Rev. D 56 (1997) 2982.

[2] L. Frankfurt, W. Koepf, M. Strikman, Phys. Rev. D 54 (1996) 3194.

[3] X. Ji, Phys. Rev. Lett. 78 (1997) 610;
X. Ji, Phys. Rev. D 55 (1997) 7114.

[4] A.V. Radyushkin, Phys. Lett. B 380 (1996) 417;
A.V. Radyushkin, Phys. Rev. D 56 (1997) 5524.

[5] D. Müller, D. Robaschik, B. Geyer, F.-M. Dittes, J. Horejsi, Fortschr. Phys. 42 (1994) 101.

[6] M. Vanderhaegen, P.A.M. Guichon, M. Guidal, Phys. Rev. Lett. 80 (1998) 5064;
M. Vanderhaegen, P.A.M. Guichon, M. Guidal, Phys. Rev. D 60 (1999) 094017.

[7] B. Mecking, et al., Nucl. Instrum. Methods A 503 (2003) 513.

[8] P. Corvisiero, et al., Nucl. Instrum. Methods A 346 (1994) 433.

[9] L.W. Mo, Y.S. Tsai, Rev. Mod. Phys. 41 (1969) 205.

[10] T.H. Bauer, et al., Rev. Mod. Phys. 50 (2) (1978) 261.

[11] K. Schilling, G. Wolf, Nucl. Phys. B 61 (1973) 381.

[12] P. Joos, et al., Nucl. Phys. B 113 (1976) 53.

[13] C. Adloff, et al., Eur. Phys. J. C 13 (2000) 371;
S. Aid, et al., Nucl. Phys. B 468 (1996) 3.

[14] J. Breitweg, et al., Eur. Phys. J. C 12 (2000) 393.

[15] A.B. Borissov, et al., HERMES Report 01-060, 2001.

[16] D.G. Cassel, et al., Phys. Rev. D 24 (1981) 2787.

[17] M. Tytgat, PhD thesis, HERMES Report 01-014, 2001.

[18] M.R. Adams, et al., Z. Phys. C 74 (1997) 237.

[19] W.D. Shambroom, et al., Phys. Rev. D 26 (1982) 1.

[20] N. Arneado, et al., Nucl. Phys. B 429 (1994) 503.

[21] F. Cano, J.-M. Laget, Phys. Lett. B 551 (2003) 317.

[22] J.-M. Laget, Phys. Lett. B 489 (2000) 313.

[23] K. Goeke, M.V. Polyakov, M. Vanderhaegen, Prog. Part. Nucl. Phys. 47 (2001) 401.

[24] M. Guidal, J.-M. Laget, M. Vanderhaeghen, Phys. Lett. B 400 (1997) 6;
M. Guidal, J.-M. Laget, M. Vanderhaeghen, Nucl. Phys. A 627 (1997) 645;
M. Guidal, J.-M. Laget, M. Vanderhaeghen, Phys. Rev. C 57 (1998) 1454;
M. Guidal, J.-M. Laget, M. Vanderhaeghen, Phys. Rev. C 61 (2000) 025204;
M. Guidal, J.-M. Laget, M. Vanderhaeghen, Phys. Rev. C 68 (2003) 058201.

[25] W.-T. Chiang, S.N. Yang, L. Tiator, M. Vanderhaeghen, D. Drechsel, Phys. Rev. C 68 (2003) 045202.

[26] J.-M. Laget, Nucl. Phys. A 699 (2002) 184.

[27] M. Battaglieri, et al., Phys. Rev. Lett. 87 (2001) 172002;
M. Battaglieri, et al., Phys. Rev. Lett. 90 (2003) 022002.

[28] A.V. Radyushkin, Phys. Rev. D 59 (1999) 014030;
A.V. Radyushkin, Phys. Lett. B 449 (1999) 81.

[29] X. Ji, J. Phys. 24 (1998) 1181.

[30] M. Polyakov, C. Weiss, Phys. Rev. D 60 (1999) 114017.

[31] A. Airapetian, et al., Eur. Phys. J. C 17 (2000) 389.

[32] P. Ball, V.M. Braun, Phys. Rev. D 54 (1996) 2182.

[33] Y. Dokshitzer, Philos. Trans. R. Soc. London A 359 (2001) 309, hep-ph/0106348.

[34] JLab experiment E99-105, spokesperons M. Garçon, M. Guidal, E. Smith.